Desalination and Water Treatment
www.deswater.com
doi: 10.1080/19443994.2015.1096829

57 (2016) 18964–18980
August

Taylor & Francis
Taylor & Francis Group

Fixed-bed column dynamics of tetracycline hydrochloride using commercial grade activated carbon: comparison of linear and nonlinear mathematical modeling studies

S. Swapna Priya*, K.V. Radha

Department of Chemical Engineering, Alagappa Chettiar College of Technology, Anna University, Chennai 600025, Tamilnadu, India, Tel. +91 9600075523; emails: swapna.athena@gmail.com (S. Swapna Priya), radhavel@yahoo.com (K.V. Radha)

Received 21 January 2015; Accepted 6 September 2015

ABSTRACT

Continuous column dynamic studies were carried out for the removal of tetracycline hydrochloride (TC-HCl) using commercial grade activated carbon. Experimental investigations were carried out for various factors such as flow rates (1.5, 3, and 5 mL min^{-1}), initial concentrations (200, 400, and 600 μg L^{-1}), and bed height (4.5, 10 cm). Experimental breakthrough curves were generated using concentration–time profile with the empirical data. The total adsorbed quantities and equilibrium uptake rates were determined by evaluating the breakthrough curves obtained at different flow rates, different initial concentrations, and different bed heights. The exhaustion time and bed capacity increased with bed height and initial concentrations and found to increase with the decrease in flow rates. The theoretical breakthrough curves were predicted using Adam–Bohart, Wolborska, Thomas, Yoon–Nelson, and Wang's model. A comparative analysis of linear and nonlinear least square methods was employed for estimating the kinetic parameters using experimental data. Error analysis was carried out for best fitting models. The results from dynamic studies showed that a maximum adsorption capacity was achieved for an initial concentration of 600 μg L^{-1} bed height of 10 cm and flow rate of 1.5 mL min^{-1}. From the kinetic models, Thomas and Yoon–Nelson model gave a better fit with linear and nonlinear regression analysis. The same was proved statistically. The nonlinear regression analysis was comparatively much better than that of linear regression analysis as observed.

Keywords: Tetracycline hydrochloride (TC-HCl); Fixed-bed reactor; Activated carbon; Mathematical modeling; Error analysis; Thomas model; Yoon–Nelson; Adam–Bohart; Wang; Wolborska

1. Introduction

Over a period of 85 years, antibiotics are considered as a part of life-saving chemical compounds globally. They are used against several bacterial and fungal infections in plants, animals, and human beings. The therapeutic use of antibiotics includes the prevention of microbial infections against (non) pathogens in human, animals, as growth promoters in agriculture, and livestock productions [1]. Though they are considered as "wonder drug" and proves to be miraculous, the vast amount of waste generated goes unknown.

*Corresponding author.

Moreover, there is no good regulation of their maximum permissible concentrations into the environment, thus it becomes tedious and inaccurate to analyze their toxicity in combination with other drug moieties [2].

Among other pharmaceutical compounds like hormones, beta-lactamide, anti-inflammatories, analgesics, lipid regulators, and anti-depressants [3], antibiotics take a special place and remain to be one of the significant causative agents for environmental pollution due to its huge consumption. Some prominent classes of antibiotics include β-lactams, tetracyclines, aminoglycoside, macrolide, glycopeptides, sulfonamides, and quinolones [4]. The transportation of antibiotics into the environment mainly comes from the bulk production unit, dosage form manufacturing unit, hospitals, and residential areas. These compounds have been present in municipal wastewater, surface water, ground water, soils, and even in drinking water, as reported in the literatures [5]. Patancheru wastewater treatment plant (WWTP), near Hyderabad, receives 1,500 m of water from 90 bulk drug manufacturers. The effluents collectively seem to contain nearly 59 pharmaceutical products. Of the 59, 11 drugs were present in very high concentrations. Antibiotics like ciprofloxacin are present at a concentration of 31,000 μg L^{-1} that can treat the entire population of Sweden for five days [6]. The occurrence and removal of 13 pharmaceuticals and 2 consumer products, including antibiotic, anti-lipidemic, anti-inflammatory, anti-hypertensive, anticonvulsant, stimulant, insect repellent, and antipsychotic, were investigated in 4 WWTPs of Beijing, China. The consumed drugs are present as (i) active agents (ii) conjugate or (iii) metabolites [7]. Hospital effluents carry urine and fecal matter of patient which contain elevated amount of unabsorbed active form of drugs like anti-inflammatory, analgesics, antibiotics, etc. Such high values of drugs will disturb the biological treatment carried out in the WWTP [8].

In the antibiotic taxonomy, tetracycline compounds were given a special focus ever since their evolution from 1948. Aureoumycin, a compound that was isolated from the soil bacteria, was the first class of tetracycline antibiotic. Semi-synthetic derivatives of tetracycline were approved by FDA in the year 1954. Second generation compounds like doxycycline and minocycline got their approvals in the year 1964 and 1971, respectively, by FDA. The third-generation tigecycline was approved in the year 2006. The mechanism of action of tetracyclines and its derivatives is initiated by attaching themselves to the ribosomal unit followed by inhibition of the translation process, hence are bacteriostatic by nature, and it is classified under broad-spectrum antibiotics [9].

Tetracycline is ranked second in the worldwide production rate and consumption rate, while China is being ranked first [10]. Globally, several thousands of tons of tetracyclines are produced annually, out of which, for veterinary purpose alone the production rate throughout the world goes in the following order in which USA has the highest production rate with 3,200 tons followed by Europe with 2,575 tons, UK with 228 tons, France 117 tons, etc. [11]. From this, it is very obvious that these compounds are prevalent for over six decades and could have been penetrated into the environment casually.

The first resistant strains towards aureomycin were reported in the year 1954 [12]. Tetracycline resistance is found to occur in three different ways, the first one being the existence and coexistence of tetracycline resistance and resistance to structurally different antibiotics giving rise to multidrug resistance, while the second type of resistance was noted to occur with ribosomal protection proteins, and the third type of resistance was found to occur by chemical inactivation, a degradative mechanism [12]. Around 12 different classes of tetracycline resistant genes have been classified (*tetA*, *tetB*, *tetC*, *tetD*, *tetE*, *tetK*, *tetL*, *tetM*, *tetO*, *tetP*, *tetQ*, *tetX*) and found to be resistant against several Gram (−ve) and Gram (+ve) bacteria [9,13].

The polar nature of tetracycline makes it more mobile and gets transported into the aquatic streams easily. The two potential ways through which the tetracycline enters the environment are through human and animal use. From human excretion, they enter the municipal sewage treatment process from where they are finally drained into the surface water and from domestic use, the landfill disposal reaches the ground water. From animal use the waste excreted becomes a source of manure for plant growth and that ultimately ends up into the food chain [11]. The occurrence of antibiotics in the environment has therefore received considerable attention. In the detection of the occurrence of antibiotics, the most frequently monitored antibiotic was tetracyclines from 80% of the wastewater samples in Wisconsin, USA [14]. Seven types of tetracyclines have been detected in surface waters in various parts of China with a residual concentration of about 1,000 ng L^{-1} [15]. About 0.14 to 50 mg kg^{-1} concentrations of tetracyclines were found in the bones of slaughtered animals [16]. They were also identified above the detection limits from the application of pig slurry to soil in a research conducted in the south of Brazil. Residual concentrations from 0.15 to 0.97 μg L^{-1} have been detected in Canada [17]. Residual concentration up to 2.37 μg L^{-1} was reported in ground water. The metabolites of chlortetracycline after 10 d were observed with a maximum concentration of up to 281,000, 157,000, and

67,000 μg kg^{-1}. Chlortetracycline has also been detected in water samples at a maximum of 0.03, 0.16, and 0.69 μg L^{-1} and concentrations up to 2,683,105, and 1,079 μg kg^{-1} of different tetracycline in soil, residual concentrations of about 183.5, 43.5, and 26.8 mg kg^{-1} of tetracycline were detected in the manure.

The threat provoked by these chemical compounds pave way for the development of several removal mechanisms that includes membrane process, adsorption process, photochemical process, electrochemical process, photocatalytic, and photoelectrocatalytic process [11]. Among several process mentioned above, adsorption is widely used process in the chemical industry especially for environmental applications due to its low cost and particularly suitable for compounds of low concentration. Adsorption process does not produce potentially more dangerous substances, and is relatively cheap in terms of initial cost, flexible, simple, and easy to operate. The solid–liquid separation process eliminates the solute particles from the liquid phase by adsorbing onto the surface of solid particles. The main reasons for considering the adsorption process in the industries are not only limited to cost-effectiveness, but also a high conversion rate is achievable per weight of the adsorbent used compared to other types of reactor.

The adsorption is operated in two modes, static and dynamic. Though static studies remains the most studied process, only continuous mode operation could give a real insight into the applicability of this technology in the industries. Dynamic adsorption is considered as an open system, where the adsorbate solution is passed continuously in the packed column [18].

Batch adsorption studies of tetracycline have been carried out onto various adsorbents like kaolinite, smectite, Palygorskite, Fe_3O_4–rGOcomposite, activated sludge, rectorite, montmorillonite, graphene oxide, aluminum oxide [19], etc., whereas continuous mode studies were carried out on activated carbon with 10 μg L^{-1} of drug concentration [20] Table 1. Though dynamic mode adsorption studies have not been much extended in the removal of tetracyclines, batch adsorption studies of TC-HCl have been realized with cGAC for high concentration solutions for acquiring equilibrium knowledge of the adsorption process [21].

The scope of the present work is to investigate the adsorption of TC-HCl on cGAC fixed-bed column in upflow manner. The consequence of the design parameters such as flow rates, bed heights, and influent concentration at fixed pH and temperature was investigated at laboratory scale. Five different mathematical models have been used in this study to analyze the behavior of the selected system. Also, linear and nonlinear methods have been used to determine the kinetic parameters and the comparison between both is revealed. The error analysis has been employed to the best fitting models.

2. Materials and methods

2.1. Reagents

Commercial grade granular activated carbon [cGAC] was bought from Sudhakar biological, Chennai, India. Tetracycline was bought in the dosage form as Tetracycline hydrochloride capsules [TC-HCl] Resteclin 250 I.P, manufactured by Abbott healthcare Pvt. Ltd, from local drug store Chennai, India. Analytical grade HCl and NaOH were purchased from Sisco Research Laboratories Pvt. Ltd, Mumbai, India. The physical and chemical properties of TC-HCl are listed in Table 2. The stock solutions of TC-HCl were prepared using reverse osmosis water (ROW) and the pH of the aqueous solution was maintained in the pH range between 6 and 6.5 using 0.1 N HCl/NaOH solutions.

2.2. Processing and characterization of cGAC for adsorption studies

At the beginning, cGAC was sieved using a mechanical sieve and the particles that were retained on the mesh of size +10/−8 were taken for further studies. The uniform-sized particles were washed with water thoroughly for several times to remove the surface adhered impurities. It was then air dried to drain off the water and the wet cGAC was kept in the hot air oven at 60˚C for about 48 h. It was then stored in an airtight container for column studies and characterization purpose. Characterization studies were conducted by BET analysis using QuadraSorb analyzer with nitrogen gas as the adsorbate, to find the surface area, pore size, and pore volume of the adsorbent The total surface area, pore volume, and average pore radius were found to be 615.917 $m^2 g^{-1}$, 0.036 cc g^{-1}, and 15.296 Å, respectively.

The FT-IR spectrum of cGAC was recorded before and after adsorption using FT-IR spectrophotometer operating in the range of 4,000–400 cm^{-1} using KBr pellet with a resolution of 1 cm^{-1}. The surface morphology by chemical alterations was examined through FT-IR analysis.

2.3. Fixed-bed adsorption studies

Fixed-bed studies were carried out in glass columns of 23 cm height with internal diameter of 7.2 cm and external diameter of 7.6 cm. A nylon mesh was placed at a height of 3.4 cm from the bottom of the

Table 1
Static and dynamic adsorption studies of tetracycline onto various adsorbents

Adsorbent	Process	pH	Refs.
Commercial grade activated carbon	Column	6.5	In this study
Coal-based carbon Coconut-based carbon	Column	6	[20]
Commercial grade activated carbon	Batch	1–7	[21]
Saline sewage Fresh water sewage	Batch	4.5–9.0	[22]
Waste tire powder	Batch	2–11	[23]
Fe–Mn binary oxide	Batch	7–8	[24]
Montmorillonite clay	Batch	6.5, 7, 7.5	[25]
Aluminum oxide	Batch	5–9	[26]
Graphene oxide	Batch	3–11	[19]
Titania and titania silica composite	Batch	4.4–9.5	[27]
Polyacrylamide cryogels	Bath	2–10	[28]
Chitosan	Batch	2.8–5.6	[29]
Swelling clay minerals	Batch	4–5	[30]
Kaolinite	Batch	3–6	[31]
Nitrifying granular sludge	Batch	7.5–8	[32]
Cinnamon soil	Batch	5–7	[33]
Fe-impregnated SBA-15	Batch	3–8	[34]
Multi-walled carbon nano tubes	Batch	5	[35]
Goethite	Batch	3–10	[36]
$MnFe_2O_4$/activated carbon magnetite composite	Batch	5	[37]
Unmodified rice straw	Batch	–	[38]

Table 2
Physical and Chemical Properties of Tetracycline Hydrochloride

Chemical name	Brand name	Formula	Molecular weight	Physical properties	Chemical properties
Tetracycline hydrochloride I.P	Restecilin	$C_{22}H_{24}N_2O_8$·HCl	480.90	Bright yellow crystalline powder pH of 2% aqueous solution around 3–3.2	Water soluble Acidic Strong oxidizing agent

reactor over which cGAC was packed. After packing the column at the desired height, the top surface was again covered with nylon mesh. The empty space above and below the column were packed with pebbles to compact the bed and to avoid dead volume spaces. The experimental setup is shown in Fig. 1. The column was operated in an up flow manner. The feed solution was pumped through peristaltic pump using intravenous tube at a uniform flow rate into the column. The samples were collected at regular intervals, stored at 4°C, and analyzed using UV–vis spectrophotometer at 360 nm. The column was desorbed completely using 0.1-N HCl solution further, in which three to four cycles of water wash was provided to ensure complete neutralization of the column before reusing.

2.4. Analysis of TC-HCl using double beam UV–vis spectrophotometer

A stock solution of tetracycline hydrochloride (TC-HCl) (1,000 μg L^{-1}) was prepared by dissolving 1 mg of TC-HCl powder taken from the pharmaceutical preparation in 1,000 mL ROW. For plotting standard curve of TC-HCl, working standard solutions of TC-HCl (100–1,000 μg L^{-1}) were prepared by diluting the stock solution to 100 mL with ROW in 100-mL volumetric flask. The concentration of TC-HCl in Resteclin capsules was analyzed spectrophtometrically [39] using double beam UV–vis spectrophotometer (UV Pharmspec 1700, Shimadzu) at 360 nm [21,28]. The same method was adopted for measuring the concentration of TC-HCl solution for column studies.

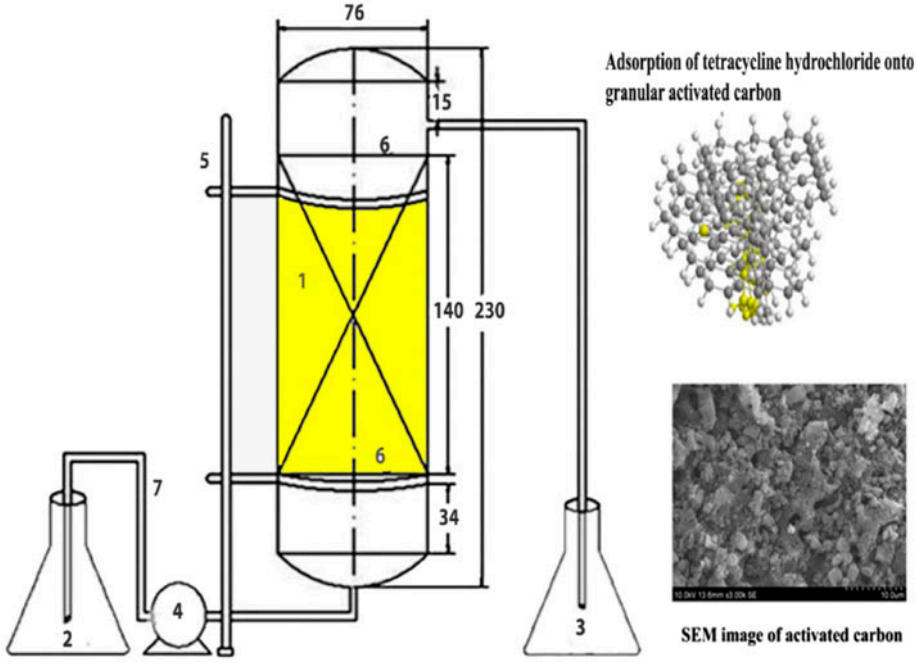

Fig. 1. Experimental setup of upflow fixed-bed reactor. All dimensions are in mm.
Notes: (1) glass column, (2) inlet feed solution vessel, (3) effluent collecting vessel, (4) peristaltic pump, (5) holding stand to support the reator, (6) nylon mesh (top and bottom), and (7) intravenous tube.

2.5. Analysis of the breakthrough curves

The packed bed column design and enhancement are tedious to describe without proper modeling especially using breakthrough curves. The column dynamics is illustrated with the help of concentration–time profile (breakthrough curves). The column performance was explained meticulously through the breakthrough curves. The shapes of the breakthrough curve as classified in the literature by [40] play an important role in the performance of the column dynamics. There are four different isotherm types, especially for organic solutes namely S, L, H, and C types, where S shape indicates a vertical orientation of the adsorbed species, L shape indicates the Langmuir isotherm model, H ("high affinity") indicates the solutes that are adsorbed as ionic micelles, and C ("constant partition") indicates that the solute easily slips into the solid surface than the solvent [40]. Breakthrough curves are vital in explaining the packed bed column studies without which the process cannot be scaled up for practical purposes. There are two ways of obtaining the breakthrough curve; one is through experimentation and the other one is obtained theoretically (modeling). The breakthrough is said to occur when the effluent concentration reaches more than 2% of the influent concentration value and bed is said to be exhausted when the effluent concentration reaches more than 95% of the influent concentration. The throughput volume of the TC-HCl solution was calculated using the following:

$$V_{\text{total}} = v \times t_{\text{total}} \tag{1}$$

where V_{total} is the volume (mL), v is the volumetric flow rate (mL min^{-1}), and t_{total} is the time (min). The total amount of TC-HCl passed through was calculated using the following:

$$m_{\text{total}} = C_{\text{i}} \times v \times t_{\text{total}}$$

where m_{total} is the amount of TC-HCl sent to the column (μg), C_{i} is the initial concentration (μg L^{-1}). The adsorption capacity was calculated using:

$$Q_{\text{ads}} = t \times v \times (C_{\text{i}} - C_{\text{f}})/M \tag{2}$$

where Q_{ads} is the adsorption capacity at the particular point in (μg g^{-1}), M is the mass of the adsorbent (g) and total adsorption capacity was calculated using:

$$Q = \sum_{t=0}^{t=t_{\text{total}}} Q_{\text{ads}} \tag{3}$$

where Q is the total amount of TC-HCl adsorbed onto cGAC in (μg g^{-1}).

2.6. Mathematical modeling

Mathematical modeling could give an exact estimation of the breakthrough curve and is used to evaluate each variable on adsorption. It is simple and can be easily realized without experimental apparatus. The liquid–solid column studies were divided into four steps that include (1) transfer of collective aggregates from the liquid phase or molecular diffusion, (2) film diffusion (interface diffusion between liquid surface and external surface of the solid), (3) interpellet mass transfer diffusion, pore diffusion, and surface diffusion and adsorption desorption reactions. For this study, five different mathematical models were used, namely Adam–Bohart's, Wolborska's, Thomas, Yoon–Nelson's, and Wang's, to ensure the rate-limiting step of the adsorption process and also to determine the kinetic parameters of column studies. The linear and nonlinear forms of those equations are listed in Table 3. Bohart and Adams described the fundamental equation describing the relationship between C/C_0 and time. The model is based on the assumption that the adsorption rate is proportional to both the residual capacity of adsorbent and concentration of the TC-HCl molecule [41–43]. Wolborska model describes the concentration distribution of a fixed bed in low concentration range of the breakthrough curve [41,44]. Thomas model is one of the most widely used theoretical models for the prediction of column breakthrough. Yoon–Nelson model is a simple model based on the assumption that the rate of decrease in the probability of adsorption for any adsorbate molecule is proportional to the probability of adsorbate adsorption and adsorbate breakthrough [41,45]. Wang developed a mass transfer model to describe the breakthrough curves assuming that the adsorption process is isothermal [18].

2.7. Error analysis

It is really critical to suggest the best fitting model as experiments and measurements are subjected to uncertainties, and also it is never possible to measure any quantities exactly. So, among the best fitting model, in order to draw meaningful conclusions, it is necessary to do error analysis. In this study, four different error analyses, namely the sum of the squares of the errors (SSE), sum of absolute errors (SAE), average relative errors (ARE), and average relative standard error (ARS) [46] were used to determine the error and the corresponding equations are listed in Table 4.

The SSE model is the most widely used error function for high concentration range and the value of error tend to increase that suggests a good fit of the respective model. The SAE is similar to that of SSE model, providing a good fit with the increase in error values. The ARE model, on the other hand tends to minimize the error studied across the entire concentration range,

Table 3
Mathematical models and equations for fixed-bed studies

Model name	Linear form	Nonlinear form	
Adam–Boharts	$\ln(C_f/C_0) = k_{ab}C_0t - k_{ab}Q_{ab}\frac{H}{v}$	$C_f/C_0 = \exp(k_{ab}C_0t - k_{ab}Q_{ab}\frac{H}{v})$	k_{ab}: kinetic constant in ml μg^{-1} min^{-1} Q_{ab}: adsorption capacity (μg g^{-1}) H: bed height in cm v: volumetric flowrate in ml min^{-1}
Wolborska	$\ln(C_f/C_0) = \frac{\beta_{wb}}{Q_{wb}}C_0t - \beta_{wb}\frac{H}{v}$	$C_f/C_0 = \exp\left(\frac{\beta_{wb}}{Q_{wb}}C_0t - \beta_{wb}\frac{H}{v}\right)$	β_{wb}: Wolborskas kinetic constant in ml μg^{-1} min^{-1} Q_{wb}: adsorption capacity in mg g^{-1}
Thomas	$\ln\left(\frac{C_0}{C_f} - 1\right) = k_{Th}Q_{Th}\frac{M}{v} - k_{Th}C_0t$	$\frac{C_f}{C_0} = \frac{1}{(1+\exp(k_{Th}Q_{Th}\frac{M}{v} - k_{Th}C_0t))}$	k_{Th}: Thomas kinetic constant in ml μg^{-1} min^{-1} Q_{Th}: adsorption capacity in mg g^{-1}
Yoon–Nelson	$\ln\left(\frac{C_f}{C_0-C_f}\right) = k_{Yn}t - k_{Yn}\tau$	$\frac{C_f}{C_0} = \frac{\exp(k_{Yn}t - k_{Yn}\tau)}{(1+\exp(k_{Yn}t - k_{Yn}\tau))}$	k_{Yn}: Yoon Nelsons kinetic constant (min^{-1}) τ: time required to reach 50% adsorbate breakthrough
Wangs	$\ln\left(\frac{C_0-C_f}{C_0}\right) = -k_w\left(t - t_{\frac{1}{2}}\right)$	$\frac{C_f}{C_0} = 1 - \exp\left(-k_w\left(t - t_{\frac{1}{2}}\right)\right)$	k_w: wangs kinetic constant (min^{-1})

Table 4
Error analysis expression

Error analysis function	Expression	Explanation
Sum of the squares of the errors	$\mathrm{SSE} = \sum_{i=1}^{n} (b_p - b_e)_i^2$	b_p and b_e is the predicted and experimental concentration ratio (C_f/C_0) with respective to Thomas and Yoon–Nelsons model
Sum of the absolute errors	$\mathrm{SAE} = \sum_{i=1}^{n} \lvert (b_p - b_e)_i \rvert$	n—number of data points
Average relative error	$\mathrm{ARE} = \frac{1}{n} \sum_{i=1}^{n} \left\lvert \frac{b_p - b_e}{b_e} \right\rvert$	
Average relative standard error	$\mathrm{ARS} = \sqrt{\sum [(b_p - b_e)/b_e]^2 / n - 1}$	

while ARS provides a meaningful comparison between the experimental and theoretical values [46,47].

3. Results and discussion

3.1. Adsorption theory of tetracycline on cGAC

Tetracycline, being an amphoteric molecule has multiple ionizable groups as shown in Fig. 2 in the aqueous solution. Depending upon the pH of the solution and adsorbent, they undergo either protonation or deprotonation reactions [31]. The experiments were carried out at solution pH (6–6.5) and it was maintained till the end of the run by the addition of buffer solutions. Tetracycline exists as zwitterions at the solution pH and the mechanism of activated carbon can be compared to that of graphite as suggested by other researchers in the adsorption of tetracycline onto various adsorbents. The mechanism of adsorption on graphene oxide was illustrated by π–π stacking interaction as a dominant driving force for the adsorption mechanisms. Another reason suggested could be of cation–π interactions. Since tetracyclines contains positively charged group in their structure, it is likely that the molecules arrange at the surface in such a way that the positively charged groups at the surface involve in cation–π bonding [19]. A similar surface reaction mechanism, π–π interaction, and carbon–π bonding was observed for tetracycline on single and multiwalled nanotubes. Rivera et al. [48] have suggested a controversial report on the mechanism of adsorption of organic compounds on activated carbons as discussed by other researchers. The adsorption mechanism involves both electrostatic and dispersive π–π adsorbent–adsorbate interactions in the adsorption of aromatic carbons. The key mechanism would be the development of hydrogen bonds between the phenolic groups of tetracycline and the oxygenated groups of carbon that influences the adsorption of TC-HCl onto cGAC [48].

3.2. Fourier transform infrared spectroscopy analysis (FT-IR)

The FT-IR spectral analysis for granular activated carbon before and after adsorption is shown in Fig. 3 that represents the variation in the functional groups. The vibrations around 3,902–3,689 cm^{-1} represent C=C stretching on virgin carbon, a sharp narrow peak is observed at band 3,446 cm^{-1} that represents the presence of –OH groups. The transmission % obtained before adsorption was seen to be in the range between 51.8 and 83.1%, except for the peak obtained at

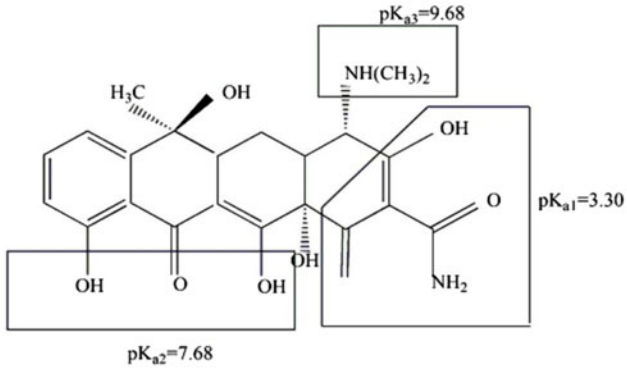

Fig. 2. Molecular structure of tetracycline with pK_a values displayed.

3,446.3 cm^{-1}, whose transmission % was 9.5. The transmission percentage after adsorption considerably reduced and it was in the range between 48.8 and 3.1%. As seen in the figure, from the left, the peak shift observed from 3,446 to 3,408 cm^{-1} represents hydrogen bond formation, the narrow peak corresponding to the respective band in the virgin carbon has been broadened and transmission rate was reduced from 9.5 to 3.1%. This indicates the –OH groups of virgin carbon and –NH groups of tetracycline had participated in the hydrogen bond formation. The band seen at 1,652.93 cm^{-1} can be assigned to amide I, while at 1,559.4 cm^{-1} correspond to amide II and N–H bending vibrations in the adsorbent [29]. The band observed at 2,361.1 cm^{-1} represents the presence of gaseous substance occupied in the pores of the adsorbent. The vibrations observed at 2,871.2, 2,809.0, 2,685.7, and 2,669.1 cm^{-1} illustrates C–H stretching. The band at 1,700 cm^{-1} indicates the inter or intramolecular hydrogen bonding formation of the –NH groups present in the tetracycline molecule. The band at 1,155 cm^{-1} indicates the asymmetric stretching of C–O–C and the band at 669.1 cm^{-1} indicates C–Cl stretching after the sorption of tetracycline on the adsorbent.

3.3. Effect of influent concentration on breakthrough curve

The consequence of influent concentration on the breakthrough curve is demonstrated in Fig. 4. As can be seen from Fig. 4 there was a decrease in the volume of adsorbate solution treated for increase in the initial concentration since high concentration caused faster transport of TC-HCl molecules due to high driving force, and also competes for the available sites. As the concentration was increased from 200 to 600 μg L^{-1}, the adsorption capacity increased from 9.9015 to 10.26^{-1} μg g^{-1} [49]. On the whole, at similar operating conditions, the adsorption capacity was found to increase with increase in the initial concentration of TC-HCl due to the fact that increased concentration levels could have caused higher diffusion and mass transfer rate between the adsorbate and adsorbent as explained by [50]. The breakthrough curves were extended for low concentration and decreased for high concentration levels that could be attributed to faster saturation levels for higher concentration than that of lower concentration levels.

3.4. Effect of flow rate on breakthrough curve

Breakthrough curves of C_f/C_0 against volume throughput are shown in Fig. 4. Flow rate is one of the important parameter in the column study. The increase/decrease in flow rate increases/decreases the contact time between the adsorbate and the adsorbent. As the contact time is increased the rate of adsorption considerably increases. The effect of TC-HCl adsorption was studied at three different flow rates (1.5, 3, 5 mL min^{-1}) for different concentrations and two different bed heights. As can been seen from Fig. 4, a comparatively quicker breakthrough was achieved at high flow rates. Also can be seen from the figure clearly that the volume treated for three different concentrations varies considerably, that is, for low concentrations 200 μg L^{-1}, the volume of effluent treated was larger than the volume treated for 600 μg L^{-1}. The adsorption rate was high initially for low flow rates obtained from empirical data since all the available sites are used effectively and liquid residence time was considerably high at low flow rates than at high flow rates. At higher flow rates, the liquid film resistance is decreased when the adsorption is subjected to external mass transfer resistance and at low-flow rates, the intraparticle mass transfer control favors the adsorption process. From Table 4, it was obvious that high-flow rates resulted in decrease of adsorption capacity for different concentrations and bed heights.

3.5. Effect of bed height on breakthrough curve

The quantity of adsorbent used plays a vital role in obtaining the breakthrough point. Different adsorbent quantity determines the bed height. The breakthrough point attained depends upon the bed height, that is, as the bed height was increased the breakthrough attained would be higher. Increase in adsorbent dosage considerably increases the surface area [51], and thereby increases the adsorption rate. For this study, two different bed heights were chosen, namely

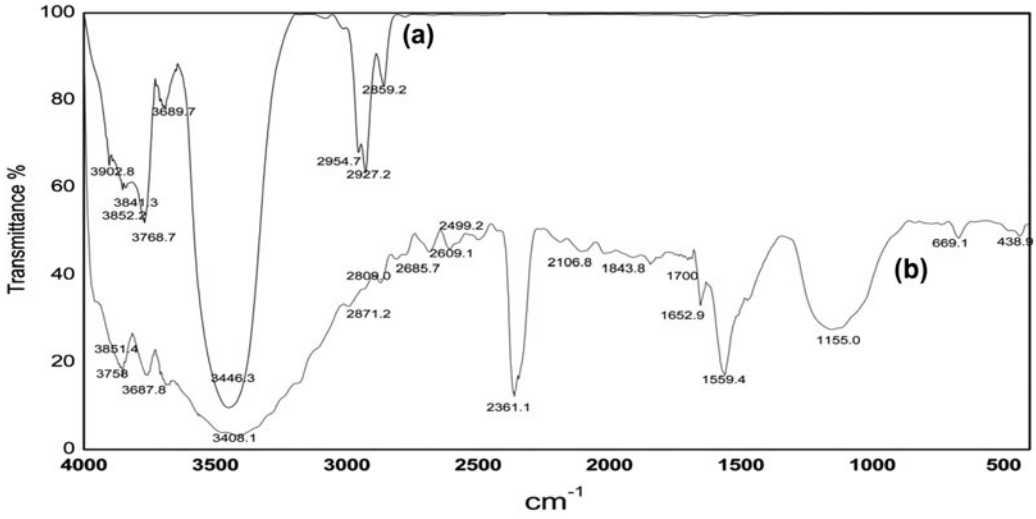

Fig. 3. FTIR analysis (a) virgin cGAC and (b) cGAC after TC-HCl adsorption.

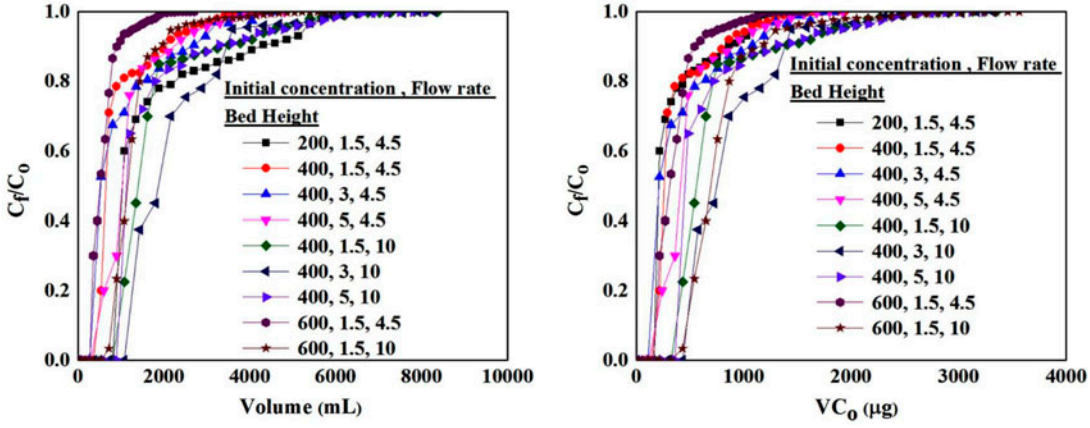

Fig. 4. Effect of initial concentration and flow rates on the breakthrough curves of TC-HCl adsorption on cGAC. Conditions: initial concentration (µg L^{-1}); flow rate (ml min^{-1}); bed height (cm), respectively.

4.5 and 10 cm, respectively. The exhaustion time increased with the increase in bed heights, as it is quite obvious that increase in adsorbent quantity would result in more active sites. The breakthrough curve is elongated for high bed heights and got shrunken for lower bed heights. The breakthrough time and saturation time increased with bed heights. The maximum adsorption capacity of 69.81 µg g^{-1} was achieved for a bed height of 10 cm and flow rate 1.5 mL min^{-1}. Thus, the adsorption capacity increased for the increase in bed heights from 4.5 to 10 cm.

3.6. Adam–Boharts model (1920)

Adam–Boharts model describes the initial part of the breakthrough curve in the continuous systems. The equations in linear and nonlinear forms are tabulated in Table 3. The equation, when rearranged, could be useful to describe the service time of the column against various bed heights. A linear and nonlinear relationship was developed using this model for the relative concentration (C_f/C_0) range greater than 0.5. From the results tabulated in Tables 6 and 7 for both linear and nonlinear model, we could see the values k_{ab} increased with the increase in concentration, flow rates, and bed heights. Moreover, the results obtained from the model were inconsistent at different operating conditions. For the linear model, the R^2 values were in the range (0.7–0.99) and for nonlinear model the R^2 values were in the range between (0.53 and 0.94). On the whole, this model did not fit well with the column data. The possible reason could be that the model behaves well for initial part of the breakthrough period. The Q_{ab} values obtained from the model were much higher than

the experimental values. In comparison to the nonlinear model, the linear model showed a better fit with the experimental data.

3.7. Wolborska model (1989)

According to this model, the assumptions made were that the breakthrough curve is controlled by film diffusion and concentration–time profile moves axially at a constant flow rate [18]. The equations pertaining to this model in the linear and nonlinear forms are tabulated in Table 3. This model has some similarities with Adam–Boharts, model as it may be suitable to explain the initial part so that the same concentrations range must be followed as that of Adam's model and moreover the results obtained would be similar to both models, except for a dissimilarity seen in the film diffusivity coefficient β_{wb} the Wolborskas constant increases with increase in concentration of bed height and flow rates. The values of regression coefficients for both non (linear) were in the range as similar to Adam–Boharts model.

3.8. Thomas model

The simple and yet most dynamic mathematical model used in prediction of breakthrough curve is Thomas model. The model was used to predict the whole length of breakthrough curve [52]. This model assumes a plug flow behavior (no axial dispersion), follows Langmuir theory, second-order reversible kinetic model and also the external and internal diffusions are negligible [53,54]. The constants were predicted from the plots that showed as the bed heights increased, the value of k_{Th} decreases. Further, for an increase in flow rate the k_{Th} increases and decreases with increase in initial concentrations as given in Tables 6 and 7. For both linear and nonlinear estimates, the same results were observed. The R^2 ranges from (0.7823 to 0.9693) for linear model, and for nonlinear the R^2 ranges from (0.96 to 0.99). The nonlinear model was found to provide a better fit in comparison to the linear model.

3.9. The Yoon–Nelson Model (1984)

This model is based on the assumption that the rate of decrease in the probability of adsorption for each adsorbate molecule is proportional to the probability of adsorbate adsorption and the probability of adsorbate breakthrough on the adsorbent [55]. The model is well suited for single component system and less complicated than other models. The linear and nonlinear forms of these equations are listed in Table 5. The value of Yoon Nelson constant increases with respect to the increase in initial concentration and decreases with bed height. The value of τ increases with the increase in concentration and bed height, and decreases with respect to the flow rate. The value of R^2 for the linear model was in the range of (0.7883–0.9674) and for nonlinear the R^2 value was in the range of (0.917–0.99). There was a similarity seen in the R^2 value obtained for Yoon–Nelson's and Thomas linear model at the respective experimental conditions, but this similarity was not observed in the nonlinear model. The adsorption capacity was calculated based on half of the total TC-HCl entering the adsorption bed with two period, which was calculated using Eq. (4) [56]. The results are tabulated in Tables 6 and 7. There was closeness in the adsorption capacity that resulted from the model and experimental conditions.

$$Q_{Yn} = \frac{C_i \times v \times \tau}{1000 \times m} \tag{4}$$

3.10. Wang's model (2003)

Wang developed a mass transfer model that was used to describe the breakthrough curve with the assumptions that the adsorption is isothermal with

Table 5
Adsorption capacity of TC-HCl onto cGAC obtained experimentally from fixed-bed studies

Initial concentration (μg L^{-1})	Flow rate (ml min^{-1})	Bed height (cm)	Adsorption capacity (μg g^{-1})
200	1.5	4.5	9.90
400	1.5	4.5	9.84
400	3	4.5	9.01
400	5	4.5	8.28
400	1.5	10	9.91
400	3	10	9.72
400	5	10	8.47
600	1.5	4.5	10.01
600	1.5	10	10.26

Table 6
Kinetic parameters obtained from five different models for fixed-bed adsorption studies of TC-HCl on cGAC (non linear model)

			Adam–Boharts model			Wolborska model			Thomas model			Yoon–Nelson model				Wangs model		
Initial concentration	Flow rate	Bed height	k_{ab}	Q_{ab}	R^2	β_{wb}	Q_{wb}	R^2	k_{Th}	Q_{Th}	R^2	k_{Yn}	Q_{Yn}	τ	R^2	k_w	$t_{1/2}$	R^2
200	1.5	4.5	0.001	23	0.84	0.026	23	0.84	0.016	9.7	0.96	0.001	11	2,937	0.98	0.001	546	0.90
400	1.5	4.5	0.008	46	0.76	0.108	46	0.76	0.045	12	0.98	0.003	16	2,084	0.98	0.002	162	0.93
400	3	4.5	0.001	33	0.56	0.055	33	0.56	0.009	12	0.96	0.007	11	686	0.99	0.004	60	0.93
400	5	4.5	0.011	13	0.94	0.373	13	0.94	0.034	12	0.96	0.013	10	394	0.99	0.006	70	0.95
400	1.5	10	0.001	48	0.64	0.061	48	0.64	0.01	10	0.99	0.002	7	2,067	0.984	0.001	197	0.99
400	3	10	0.004	43	0.80	0.187	43	0.80	0.01	10	0.99	0.001	13	1,815	0.917	0.002	208	0.94
400	5	10	0.014	26	0.74	0.370	26	0.74	0.01	10	0.97	0.013	11	926	0.99	0.005	90	0.91
600	1.5	4.5	0.001	24	0.53	0.034	24	0.53	0.02	10	0.99	0.012	10	872	0.98	0.003	109	0.95
600	1.5	10	0.004	33	0.86	0.127	33	0.86	0.03	11	0.99	0.004	10	1,825	0.98	0.002	254	0.92

Table 7
Kinetic parameters obtained from five different models for fixed-bed adsorption studies of TC-HCl on cGAC (Linear model)

			Adam–Boharts model			Wolborska model			Thomas model			Yoon–Nelson model				Wangs model		
Initial concentration	Flow rate	Bed height	k_{ab}	Q_{ab}	R^2	β_{wb}	Q_{wb}	R^2	k_{Th}	Q_T	R^2	k_{Yn}	τ	Q_{Yn}	R^2	k_w	$t_{1/2}$	R^2
200	1.5	4.5	0.002	17	0.89	0.002	17	0.89	0.007	9	0.78	0.001	1,162	4.5	0.78	0.001	524	0.75
400	1.5	4.5	0.014	10	0.80	0.014	10	0.80	0.006	12	0.92	0.002	621	4.4	0.92	0.002	227	0.91
400	3	4.5	0.004	19	0.87	0.004	19	0.87	0.009	11	0.93	0.003	231	4.2	0.93	0.003	117	0.91
400	5	4.5	0.027	16	0.95	0.027	16	0.95	0.020	12	0.86	0.008	201	5.2	0.93	0.007	98	0.94
400	1.5	10	0.032	10	0.99	0.032	10	0.99	0.003	10	0.92	0.001	858	3.2	0.92	0.001	366	0.93
400	3	10	0.004	38	0.88	0.004	38	0.88	0.007	9	0.96	0.003	596	4.4	0.96	0.002	349	0.97
400	5	10	0.002	38	0.90	0.002	38	0.90	0.011	9	0.90	0.004	290	2.1	0.90	0.004	105	0.88
600	1.5	4.5	0.005	15	0.95	0.005	15	0.95	0.010	10	0.93	0.006	458	5.5	0.93	0.005	275	0.91
600	1.5	10	0.006	30	0.74	0.006	30	0.74	0.004	10	0.89	0.002	685	3.8	0.90	0.002	303	0.96

symmetrical breakthrough, and negligible axial dispersion for the mass transfer model (Eq. (5)) in which x is the fraction of adsorbed adsorbates and y is the fraction of adsorbate passing through the bed by assuming $x + y = 1$ [18]. The linear and nonlinear forms of the equations are tabulated and from the Wang plot the values of the kinetic constants were evaluated. The model looks somewhat similar to Yoon–Nelson's model but fails to provide as much as information as the former model could provide in the adsorption studies. The entire breakthrough curve could be generated from Wang equation. The Wang constant k_w was found to increase with increase in flow rates but decreased with bed heights. The values of $t_{1/2}$ decreased with increase in flow rates as given in table. The R^2 value lied in the range of 0.76–0.901 for nonlinear model and for linear model the R^2 values were greater than 0.9. Thus, from the results of Wang's model, the bed was assumed to behave in a plug flow manner [18].

$$-\frac{dy}{dt} = k_w xy \tag{5}$$

3.11. Breakthrough curve analysis

The Thomas and Yoon–Nelson's parameters obtained using linear and nonlinear regression model were used to generate theoretical breakthrough curves and the obtained curves were compared with the experimental breakthrough curves. As can been seen in Fig. 5, the experimental and predicted breakthrough curves almost overlap except for the nonlinear Yoon–Nelson model. The entire breakthrough

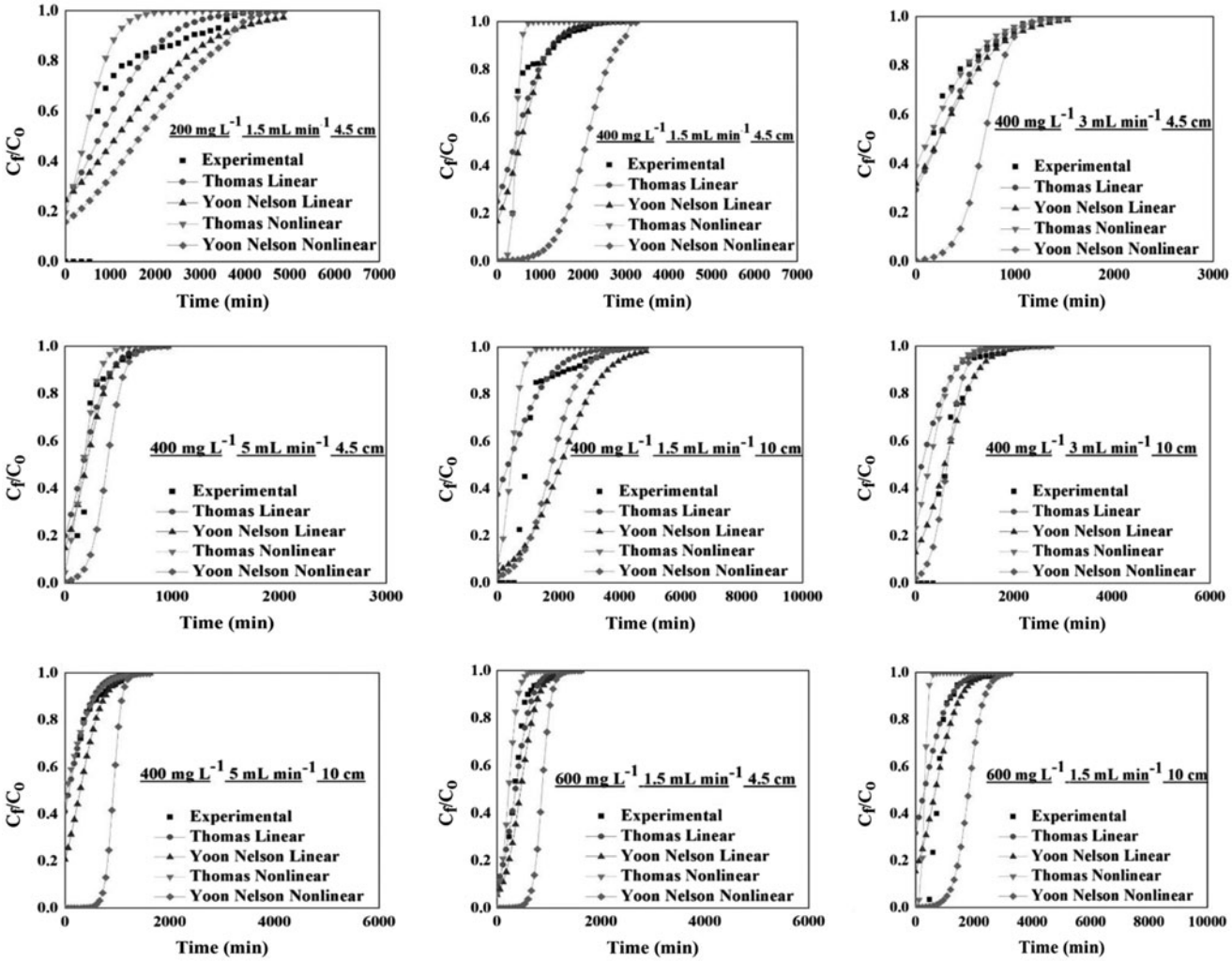

Fig. 5. Comparison of linear, nonlinear predicted and experimental breakthrough curves for TC-HCl adsorption onto cGAC packed column using Thomas and Yoon–Nelsons model at various initial concentrations, flow rates and bed heights, respectively.

Table 8
Error analysis values

	Thomas Model								Yoon–Nelson Model							
	Linear				Nonlinear				Linear				Nonlinear			
Initial concentration (μg L^{-1})	SAE	SSE	ARE	ARS	SAE	SSE	ARE	ARS	SAE	SSE	ARE	ARS	SAE	SSE	ARE	ARS
200	0.833	0.479	0.024	0.086	5.00	2.27	0.1335	0.1785	0.833	0.478	0.024	0.079	3.58	1.19	0.089	0.110
400	0.719	0.456	0.028	0.076	0.45	0.452	0.022	0.169	0.719	0.456	0.028	0.076	12.27	9.57	0.569	0.692
400	0.237	0.265	0.019	0.049	0.954	0.378	0.009	0.022	0.870	0.407	0.001	0.018	3.96	2.15	0.238	0.418
400	0.694	0.236	0.018	0.054	0.118	0.076	0.009	0.084	0.297	0.167	0.030	0.078	2.68	1.219	0.183	0.348
400	2.851	1.146	0.096	0.369	3.932	1.391	0.200	0.576	1.260	0.610	0.029	0.241	3.43	1.466	0.187	0.363
400	3.655	1.564	0.132	0.303	3.099	1.026	0.125	0.271	1.113	0.317	0.016	0.078	1.48	0.44	0.033	0.112
400	2.423	1.084	0.014	0.025	2.539	1.278	0.013	0.0243	1.424	0.731	0.014	0.045	2.33	1.46	0.133	0.340
600	0.375	0.152	0.014	0.045	2.062	0.561	0.123	0.257	0.362	0.161	0.014	0.047	7.97	5.29	0.397	0.604
600	3.298	1.369	0.664	3.118	4.446	2.507	1.119	5.044	0.880	0.467	0.354	1.881	8.13	5.09	0.360	0.549

curve obtained from nonlinear Yoon–Nelson's model was highly symmetrical and takes "S" shape that shows a vertical orientation of the adsorbed TC-HCl molecules. From the breakthrough curves obtained, Yoon–Nelson and Thomas model was found to give a best fit to the experimental data. This also indicates the applicability of these two models in the prediction of column dynamics of TC-HCl onto cGAC.

3.12. Error analysis

Due to existence of experimental limitations and deviations from practical errors arising from the system would result in assorted form of parameter values and distortion in fits. Error functions are applied to identify the extent of deviation [46]. In this study, four different error analyses were applied to two models namely Thomas and Yoon–Nelson model for both linear and nonlinear results. The error values (SSE, SAE, ARE, ARS) obtained for linear and nonlinear Thomas and Yoon Nelson's model are tabulated in Table 8. The values were found to decrease with the increase in initial concentrations, flow rate, and bed heights. The way in which the results were obtained was similar to both linear and nonlinear models of Thomas and Yoon–Nelson. Furthermore, the error values obtained for the linearized Thomas model was found to be higher than that of the nonlinear model, whereas for the Yoon–Nelson's model the error values were found to be higher for nonlinear model than that of linear model. The nonlinear error analysis in contrast to the linear mode involves either in the minimization or maximization of the predicted values based on its convergence criteria.

4. Conclusion

Continuous column studies in the adsorption of TC-HCl onto cGAC were successfully carried out at different initial concentrations, flow rates, and bed heights. The experimental data were modeled using five different models, namely Adam–Boharts, Wolborska, Thomas, Yoon–Nelson and Wang's model. The adsorption capacity was found to increase with increase in initial concentration, bed heights, and decreases with increase in flow rates. Adam–Boharts model was used to describe the initial part of the breakthrough curve and Wolborska was attempted to check whether the resistance to adsorption process was controlled by film diffusion, while Thomas and Wangs model were attempted to prove plug flow behavior of the bed and Yoon–Nelson's model was exclusively used for single component and used to determine the time required to achieve 50% adsorbate breakthrough. The data were compared using linear and nonlinear regression model equations, parameters obtained using linearization isotherm models would be inappropriate as they would be focused on the points around the line following a Gaussian distribution and the error distribution would be uniform at every value of the adsorbate concentration, whereas adsorption isotherms are always nonlinear and they get altered when linearized. The coefficient of determination obtained using nonlinear regression was higher than that of the linear distribution. The error analysis was carried out to two good fitting models to know the best fitting model.

Symbols

V_{total}	—	total volume (mL)
V	—	volumetric flow rate (mL min^{-1})
t_{total}, t	—	TIME (min)
m_{total}	—	total amount of tetracycline hydrochloride sent to the column (μg)
C_0, C_f	—	initial and final concentration of tetracycline hydrochloride solution (μg L^{-1})
Q, Q_{ads}, Q_{ab}, Q_{wb}, Q_{Th}, Q_{Yn}	—	adsorption capacity (μg g^{-1})
M	—	mass of the adsorbent (g)
SSE	—	sum of the squares of the errors
SAE	—	sum of absolute errors
ARE	—	average relative errors
ARS	—	average relative standard errors
cGAC	—	commercial grade granular activated carbon
TC-HCl	—	tetracycline hydrochloride
k_{ab}	—	Adam–Boharts kinetic constant (ml μg^{-1} min^{-1})
β_{wb}	—	Wolborskas kinetic constant (ml μg^{-1} min^{-1})
k_{Th}	—	Thomas kinetic constant (ml μg^{-1} min^{-1})
k_W	—	Wangs kinetic constant (min^{-1})
τ	—	time required to reach 50% adsorbate breakthrough (min)

References

[1] A.L. Batt, D.S. Aga, Simultaneous analysis of multiple classes of antibiotics by ion trap LC/MS/MS for assessing surface water and groundwater contamination, Anal. Chem. 77 (2005) 2940–2947.

[2] J.D. Méndez-Díaz, G. Prados-Joya, J. Rivera-Utrilla, R. Leyva-Ramos, M. Sánchez-Polo, M.A. Ferro-García, N.A. Medellín-Castillo, Kinetic study of the adsorption of nitroimidazole antibiotics on activated carbons in aqueous phase, J. Colloid Interface Sci. 345 (2010) 481–490.

[3] N. Kulik, M. Trapido, A. Goi, Y. Veressinina, R. Munter, Combined chemical treatment of pharmaceutical effluents from medical ointment production, Chemosphere 70 (2008) 1525–1531.
[4] K. Kümmerer, Antibiotics in the aquatic environment—A review—Part I, Chemosphere 75 (2009) 417–434.
[5] R. Lindberg, P.A. Jarnheimer, B. Olsen, M. Johansson, M. Tysklind, Determination of antibiotic substances in hospital sewage water using solid phase extraction and liquid chromatography/mass spectrometry and group analogue internal standards, Chemosphere 57 (2004) 1479–1488.
[6] D.J. de Pedro, C. Larsson, N. Paxeus, Effluent from drug manufactures contains extremely high levels of pharmaceuticals, J. Hazard. Mater. 148 (2007) 751–755.
[7] Q. Sui, J. Huang, S. Deng, G. Yu, Q. Fan, Occurrence and removal of pharmaceuticals, caffeine and DEET in wastewater treatment plants of Beijing, China, Water Res. 44 (2009) 417–426.
[8] K.H. Langford, K.V. Thomas, Determination of pharmaceutical compounds in hospital effluents and their contribution to wastewater treatment works, Environ. Int. 35 (2009) 766–770.
[9] B.S. Speer, N.B. Shoemaker, A.A. Salyers, Bacterial resistance to tetracycline: Mechanisms, transfer, and clinical significance, Clin. Microbial. Rev. 5 (1992) 387–399.
[10] X. Xie, Q. Zhou, Z. He, Y. Bao, Physiological and potential genetic toxicity of chlortetracycline as an emerging pollutant in wheat (*Triticum aestivum* L.), Environ. Toxicol. Chem. 29 (2010) 922–928.
[11] R. Daghrir, P. Drogui, Tetracycline antibiotics in the environment: A review, Environ. Chem. Lett. 11 (2013) 209–227.
[12] M.L. Nelson, S.B. Levy, The history of the tetracyclines, Ann. N.Y. Acad. Sci. 1241 (2011) 17–32.
[13] I. Chopra, M. Roberts, Tetracycline antibiotics: Mode of action, applications, molecular biology, and epidemiology of bacterial resistance, Microbiol. Mol. Biol. Rev. 65 (2001) 232–260.
[14] K.G. Karthikeyan, M.T. Meyer, Occurrence of antibiotics in wastewater treatment facilities in Wisconsin, USA, Mater. Chem. Phys. 361 (2006), 196–207.
[15] Q. Bu, B. Wang, J. Huang, S. Deng, G. Yu, Pharmaceuticals and personal care products in the aquatic environment in China: A review, J. Hazard. Mater. 262 (2013) 189–211.
[16] M. Kühne, S. Wegmann, A. Kobe, R. Fries, Tetracycline residues in bones of slaughtered animals, Food Control 11 (2000) 175–180.
[17] X.S. Miao, F. Bishay, M. Chen, C.D. Metcalfe, Occurrence of antimicrobials in the final effluents of wastewater treatment plants in Canada, Environ. Sci. Technol. 38 (2004) 3533–3541.
[18] Z. Xu, J.G. Cai, B.C. Pan, Mathematically modeling fixed-bed adsorption in aqueous systems, Appl. Phys. Eng. 14 (2013) 155–176.
[19] Y. Gao, Y. Li, L. Zhang, H. Huang, J. Hu, S.M. Shah, X. Su, Adsorption and removal of tetracycline antibiotics from aqueous solution by graphene oxide, J. Colloid Interface Sci. 368 (2012) 540–546.
[20] K.J. Choi, S.G. Kim, S.H. Kim, Removal of antibiotics by coagulation and granular activated carbon filtration, J. Hazard. Mater. 151 (2008) 38–43.
[21] S. Swapna Priya, K.V. Radha, Equilibrium, isotherm, kinetic and thermodynamic adsorption studies of tetracycline hydrochloride onto commercial grade granular activated carbon, Int. J. Pharm. Pharm. Sci. 7 (2015) 42–51.
[22] B. Li, T. Zhang, Removal mechanisms and kinetics of trace tetracycline by two types of activated sludge treating freshwater sewage and saline sewage, Environ. Sci. Pollut. Res. 20 (2013) 3024–3033.
[23] F. Lian, Z. Song, Z. Liu, L. Zhu, B. Xing, Mechanistic understanding of tetracycline sorption on waste tire powder and its chars as affected by Cu^{2+} and pH, Environ. Pollut. 178 (2013) 264–270.
[24] H. Liu, Y. Yang, J. Kang, M. Fan, J. Qu, Removal of tetracycline from water by Fe–Mn binary oxide, J. Environ. Sci. 24 (2012) 242–247.
[25] D. Avisar, O. Primor, I. Gozlan, H. Mamane, Sorption of sulfonamides and tetracyclines to montmorillonite clay, Water, Air, Soil Pollut. 209 (2010) 439–450.
[26] W.R. Chen, C.H. Huang, Adsorption and transformation of tetracycline antibiotics with aluminum oxide, Chemosphere 79 (2010) 779–785.
[27] M. Brigante, P.C. Schulz, Remotion of the antibiotic tetracycline by titania and titania–silica composed materials, J. Hazard. Mater. 192 (2011) 1597–1608.
[28] E. Bağda, M. Erşan, E. Bağda, Investigation of adsorptive removal of tetracycline with sponge like, *Rosa canina* gall extract modified, polyacrylamide cryogels, J. Environ. Chem. Eng. 1 (2013) 1079–1084.
[29] J. Kang, H. Liu, Y.M. Zheng, J. Qu, J.P. Chen, Systematic study of synergistic and antagonistic effects on adsorption of tetracycline and copper onto a chitosan, J. Colloid Interface Sci. 344 (2010) 117–125.
[30] P.H. Chang, Z. Li, W.T. Jiang, J.S. Jean, Adsorption and intercalation of tetracycline by swelling clay minerals, Appl. Clay Sci. 46 (2009) 27–36.
[31] Y. Zhao, J. Geng, X. Wang, X. Gu, S. Gao, Tetracycline adsorption on kaolinite: pH, metal cations and humic acid effects, Ecotoxicology 20 (2011) 1141–1147.
[32] Y.J. Shi, X.H. Wang, Z. Qi, M.H. Diao, M.M. Gao, S.F. Xing, S.G. Wang, X.C. Zhao, Sorption and biodegradation of tetracycline by nitrifying granules and the toxicity of tetracycline on granules, J. Hazard. Mater. 191 (2011) 103–109.
[33] Y. Wan, Y. Bao, Q. Zhou, Simultaneous adsorption and desorption of cadmium and tetracycline on cinnamon soil, Chemosphere 80 (2010) 807–812.
[34] B.K. Vu, E.W. Shin, O. Snisarenko, W.S. Jeong, H.S. Lee, Removal of the antibiotic tetracycline by Fe-impregnated SBA-15, Korean J. Chem. Eng. 27 (2010) 116–120.
[35] L. Ji, W. Chen, J. Bi, S. Zheng, Z. Xu, D. Zhu, P.J. Alvarez, Adsorption of tetracycline on single-walled and multi-walled carbon nanotubes as affected by aqueous solution chemistry, Environ. Toxicol. Chem. 29 (2010) 2713–2719.
[36] Y. Zhao, J. Geng, X. Wang, X. Gu, S. Gao, Adsorption of tetracycline onto goethite in the presence of metal cations and humic substances, J. Colloid Interface Sci. 361 (2011) 247–251.
[37] L. Shao, Z. Ren, G. Zhang, L. Chen, Facile synthesis, characterization of a $MnFe_2O_4$/activated carbon magnetic composite and its effectiveness in tetracycline removal, Mater. Chem. Phys. 135 (2012) 16–24.

[38] S. Swapna Priya, K.V. Radha, D. Kheerthana, Batch biosorption studies of tetracycline hydrochloride onto unmodified rice straw: Equilibrium, kinetic and thermodynamic studies, Bioresour. Technol. 6 (2014) 6, 4709–4721.
[39] S. Swapna Priya, K.V. Radha, Brief review of spectrophotometric methods for the detection of tetracycline antibiotics, Int. J. Pharm. Pharm. Sci. 6 (2014) 48–51.
[40] C. Giles, T. MacEwan, S.N. Nakhwa, Studies in adsorption. Part XI. A system of classification of solution adsorption isotherms, and its use in diagnosis of adsorption mechanisms and in measurement of specific surface areas of solids, J. Chem. Soc. (Resumed) 786 (1960) 3973–3993.
[41] M. Goyal, M. Bhagat, Dynamic adsorption of Pb(II) ions from aqueous solution using activated carbon beds, Indian. J. Eng. Mater. Sci. 17 (2010) 367–372.
[42] G. Bohart, E.Q. Adams, Some aspects of the behaviour of charcoal with respect to chlorine, J. Am. Chem. Soc. 4 (2010) 523–544.
[43] A. Wolborska, Adsorption on activated carbon of p-nitrophenol from aqueous solution, Water Res. 23 (1989) 85–91.
[44] A. Ghribi, M. Chlendi, Modeling of fixed bed adsorption: Application to the adsorption of an organic dye, Asian J. Text. 1 (2011) 161–171.
[45] Y.H. Yoon, J.H. Nelson, Application of gas adsorption kinetics-II. A theoretical model for respirator cartridge service life and its practical applications, Am. Ind. Hyg. Assoc. J. 45 (1984) 517–524.
[46] R. Han, Y. Wang, W. Zou, Y. Wang, J. Shi, Comparison of linear and nonlinear analysis in estimating the Thomas model parameters for methylene blue adsorption onto natural zeolite in fixed-bed column, J. Hazard. Mater. 145 (2007) 331–335.
[47] K.Y. Foo, B.H. Hameed, Insights into the modeling of adsorption isotherm systems, Chem. Eng. J. 156 (2010) 2–10.
[48] J. Rivera-Utrilla, C.V. Gómez-Pacheco, M. Sánchez-Polo, J.J. López-Peñalver, R. Ocampo-Pérez, Tetracycline removal from water by adsorption/bioadsorption on activated carbons and sludge-derived adsorbents, J. Environ. Manage. 131 (2013) 16–24.
[49] M. Tamez Uddin, M. Rukanuzzaman, M.M.R. Khan, M.A. Islam, Adsorption of methylene blue from aqueous solution by jackfruit (*Artocarpus heteropyllus*) leaf powder: A fixed-bed column study, J. Environ. Manage. 90 (2009) 3443–3450.
[50] N. Chen, Z.Y. Zhang, C.P. Feng, M. Li, R.Z. Chen, N. Sugiura, Investigations on the batch and fixed-bed column performance of fluoride adsorption by Kanuma mud, Desalination 268 (2011a) 76–82.
[51] E. Malkoc, Y. Nuhoglu, Removal of Ni(II) ions from aqueous solutions using waste tea factory: Adsorption on a fixed bed column, J. Hazard. Mater. 135 (2006) 328–336.
[52] D. Kumar, S.S. Sambi, S.K. Sharma, V. Kumar, Removal of nickel ions from aqueous solutions on packed bed of zeolite NaX, Chem. Eng. Trans. 11 (2007) 191.
[53] B. Ahmad Albadarin, C. Mangwandi, H. Alaa Al-Muhtaseb, M. Gavin Walker, J. Stephen Allen, N.M. Mohammad Ahmad, Modelling and fixed bed column adsorption of Cr(VI) onto orthophosphoric acid activated lignin, Chinese, J. Chem. Eng. 20 (2012) 469–477.
[54] S. Chen, Q. Yue, B. Gao, Q. Li, X. Xu, K. Fu, Adsorption of hexavalent chromium from aqueous solution by modified corn stalk: A fixed-bed column study, Bioresour. Technol. 113 (2012) 114–120.
[55] N. Öztürk, D. Kavak, Boron removal from aqueous solutions by adsorption on waste sepiolite and activated waste sepiolite using full factorial design, Adsorption 10 (2004) 245–257.
[56] P. Sivakumar, P.N. Palaniswamy, Packed bed column studies for the removal of acid blue 92 and basic red 29 using non-conventional adsorbent, Indian. J. Chem. Technol. 16 (2009) 301–307.